Supplementary Information

Discovery of an α-Aminophosphonic acid VIM-2 Inhibitor

Kinga Virág Gulyás, Kim Bartels, Gurleen Kaur, Sahar Najam, Zoltán Palczert, Viola Tamási, Karina Calvopina Tapia, Anna Andersson Rasmussen, Máté Simon, Johannes Thoma, Miklós Csala, Christopher J. Schofield, Eike C. Schulz, and Máté Erdélyi

Table of Contents

1. NMR spectra

Diethyl ((benzylamino)(2-methoxyphenyl)methyl)phosphonate (1)

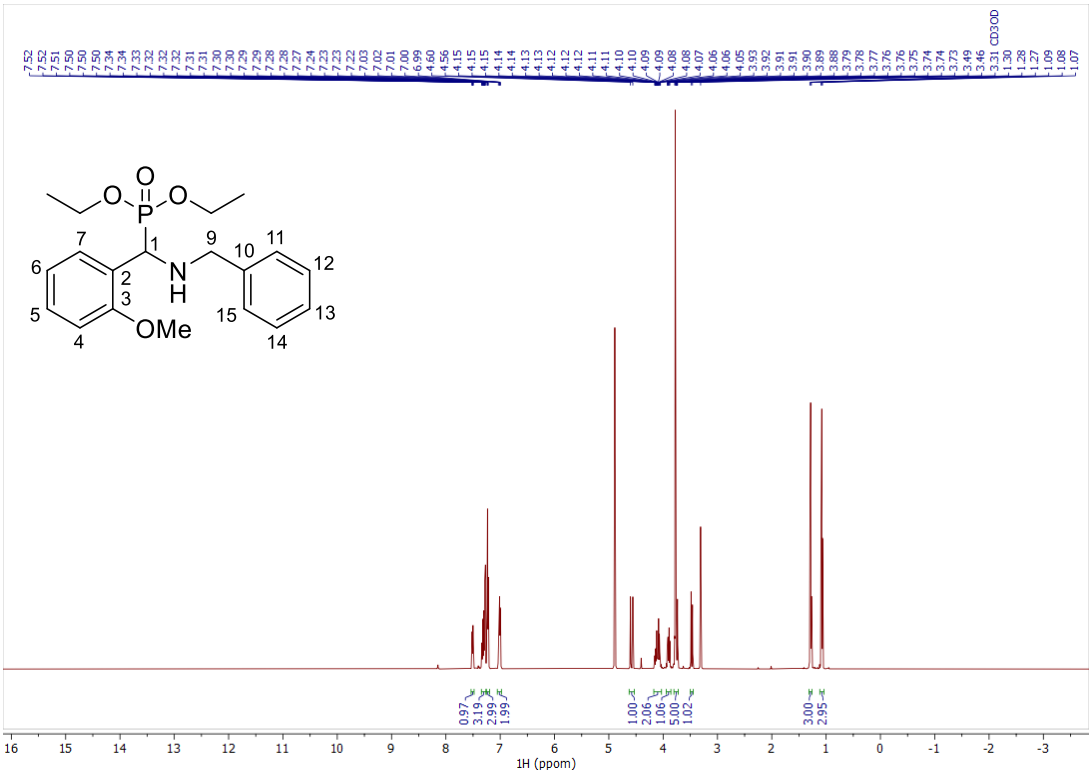

Figure S1. *^{1}H NMR spectrum of **1** (500 MHz, CD_3OD).*

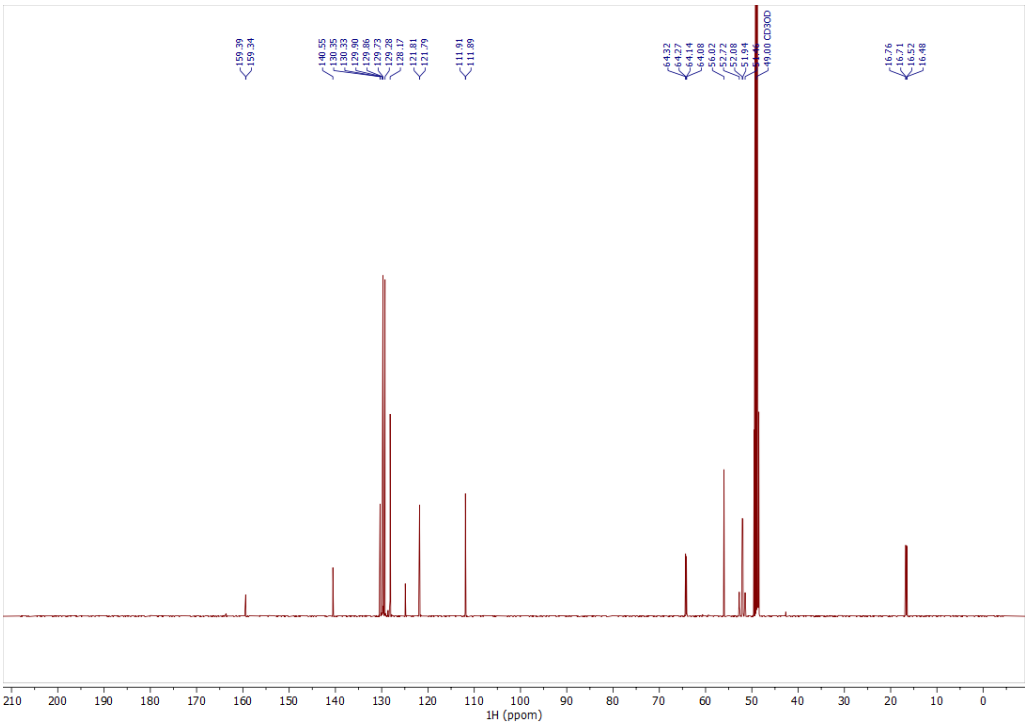

Figure S2. *^{13}C NMR spectrum of **1** (500 MHz, CD_3OD).*

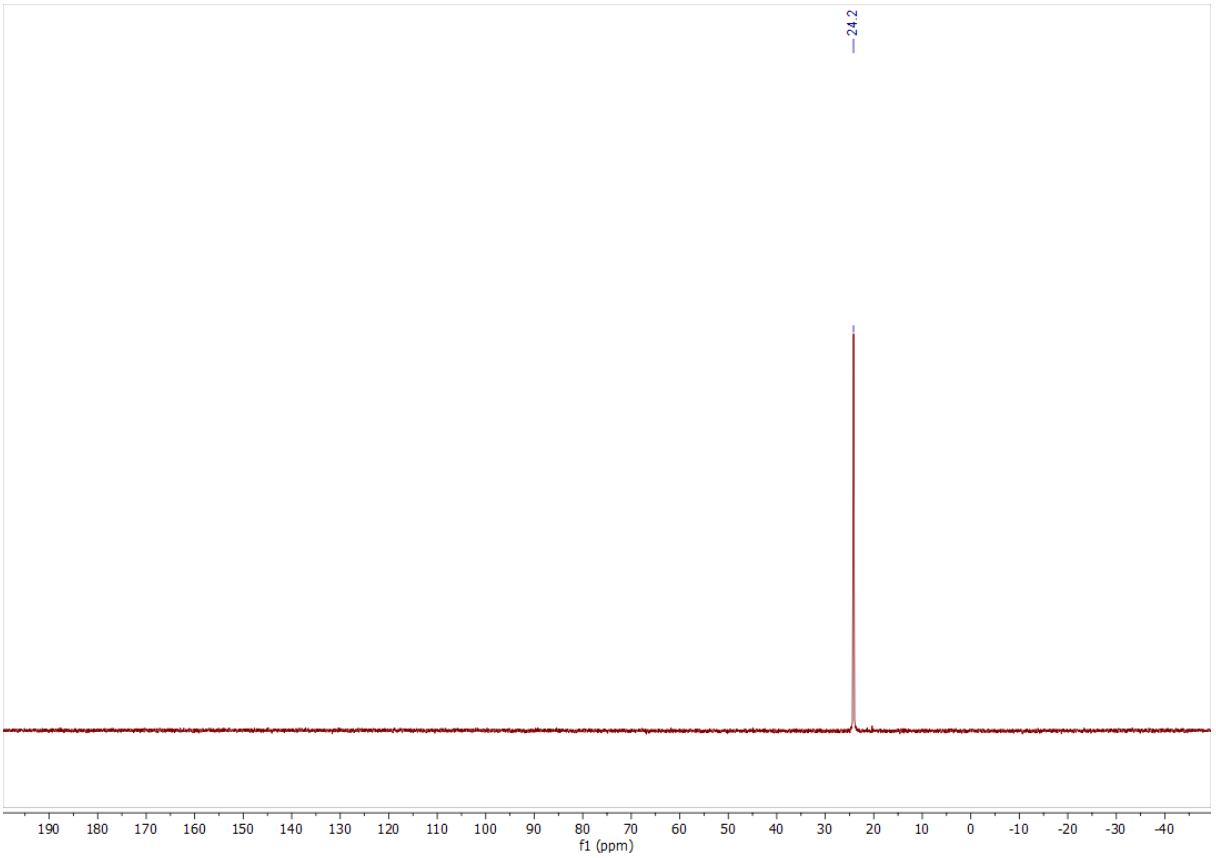

Figure S3. *^{31}P NMR spectrum of **1** (400 MHz, CD_3OD).*

Diethyl ((benzylamino)(pyridin-2-yl)methyl)phosphonate (2)

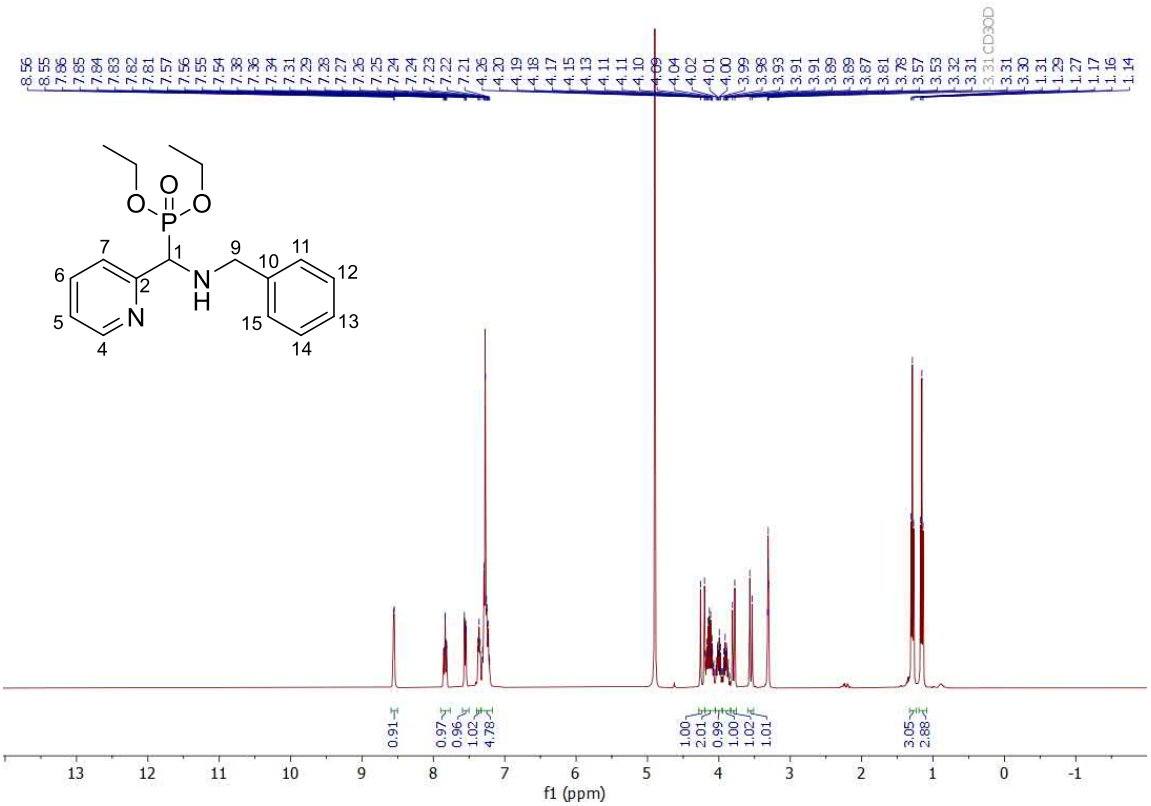

Figure S4. *^{1}H NMR spectrum of **2** (400 MHz, CD_3OD).*

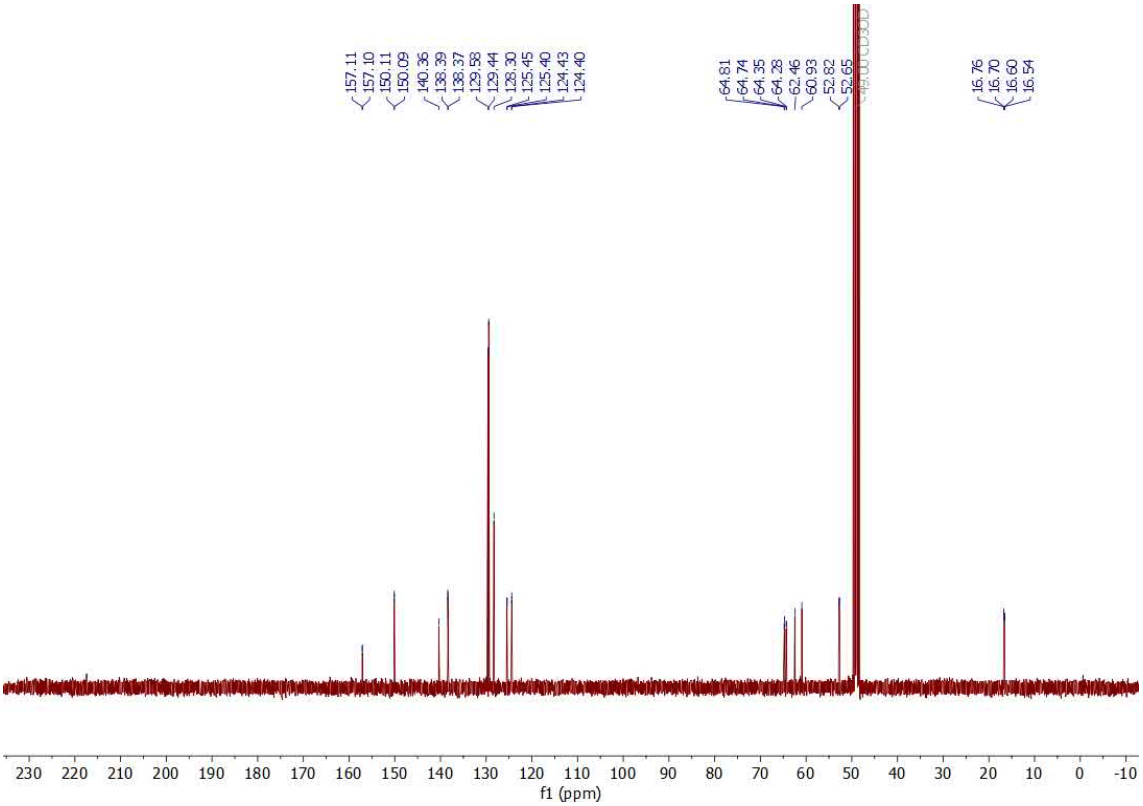

Figure S5. *^{13}C NMR spectrum of **2** (500 MHz, CD_3OD).*

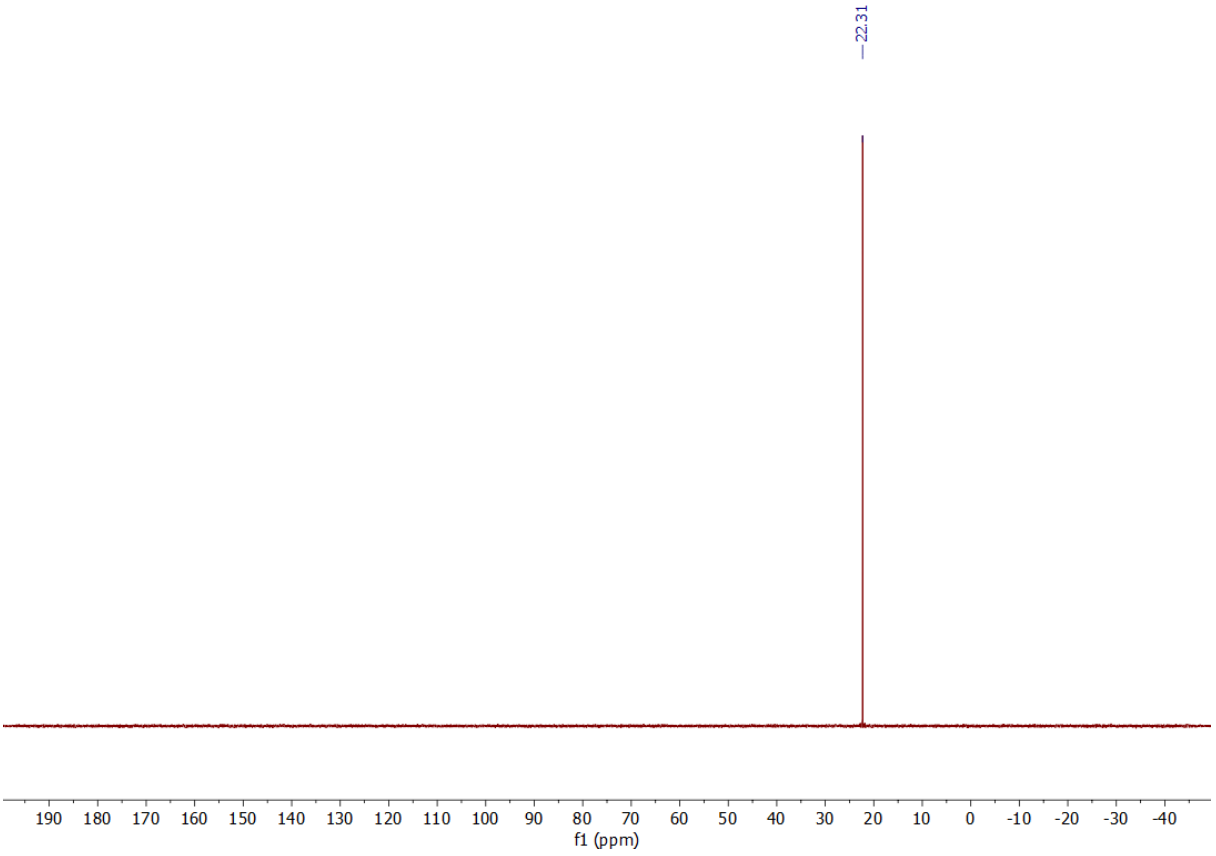

Figure S6. *^{31}P NMR spectrum of **2** (400 MHz, CD_3OD).*

Diethyl (amino(2-methoxyphenyl)methyl)phosphonate (3)

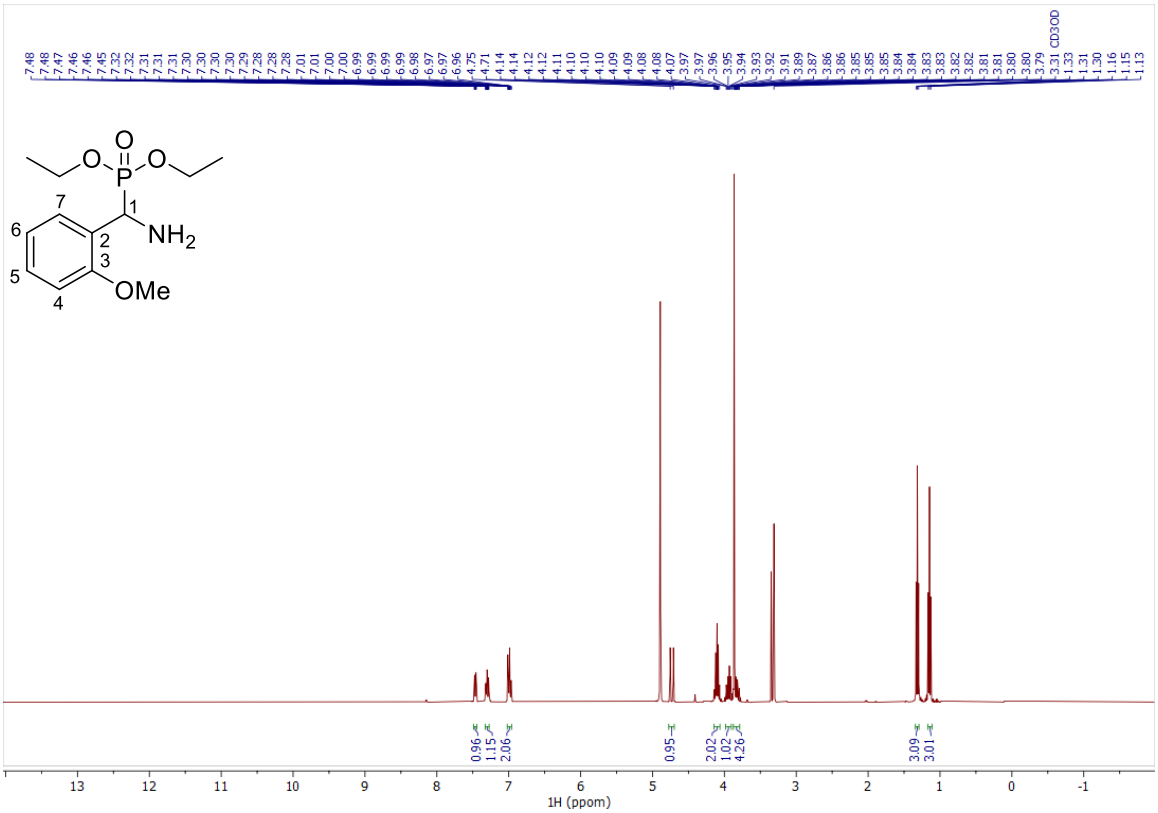

Figure S7. *^{1}H NMR spectrum of **3** (400 MHz, CD_3OD).*

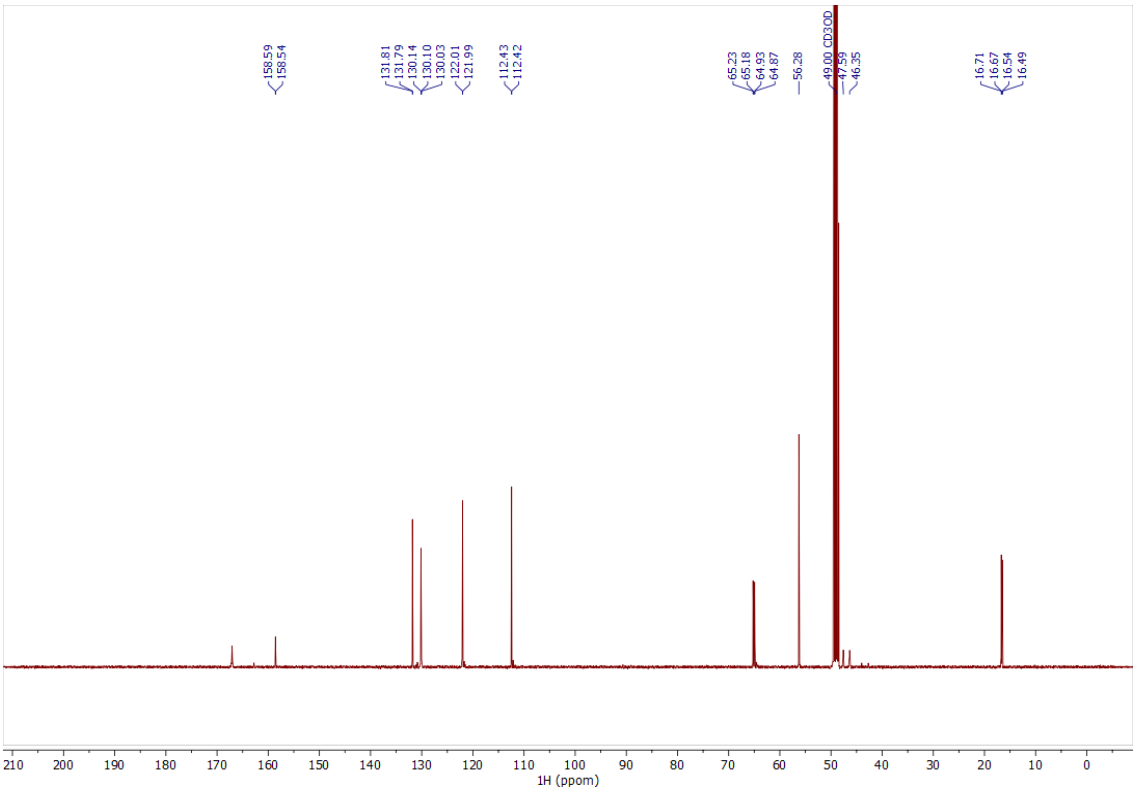

Figure S8. *^{13}C NMR spectrum of **3** (500 MHz, CD_3OD).*

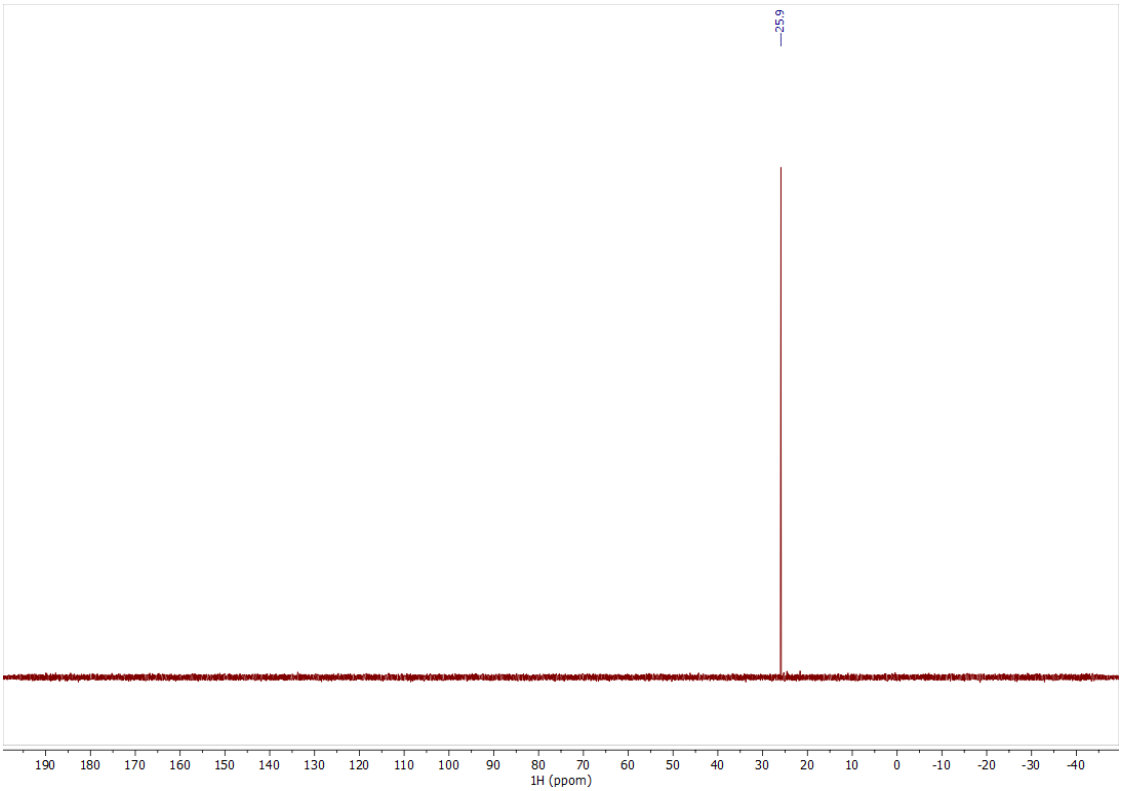

Figure S9. *^{31}P NMR spectrum of **3** (400 MHz, CD_3OD).*

(Amino(2-hydroxyphenyl)methyl)phosphonic acid (4)

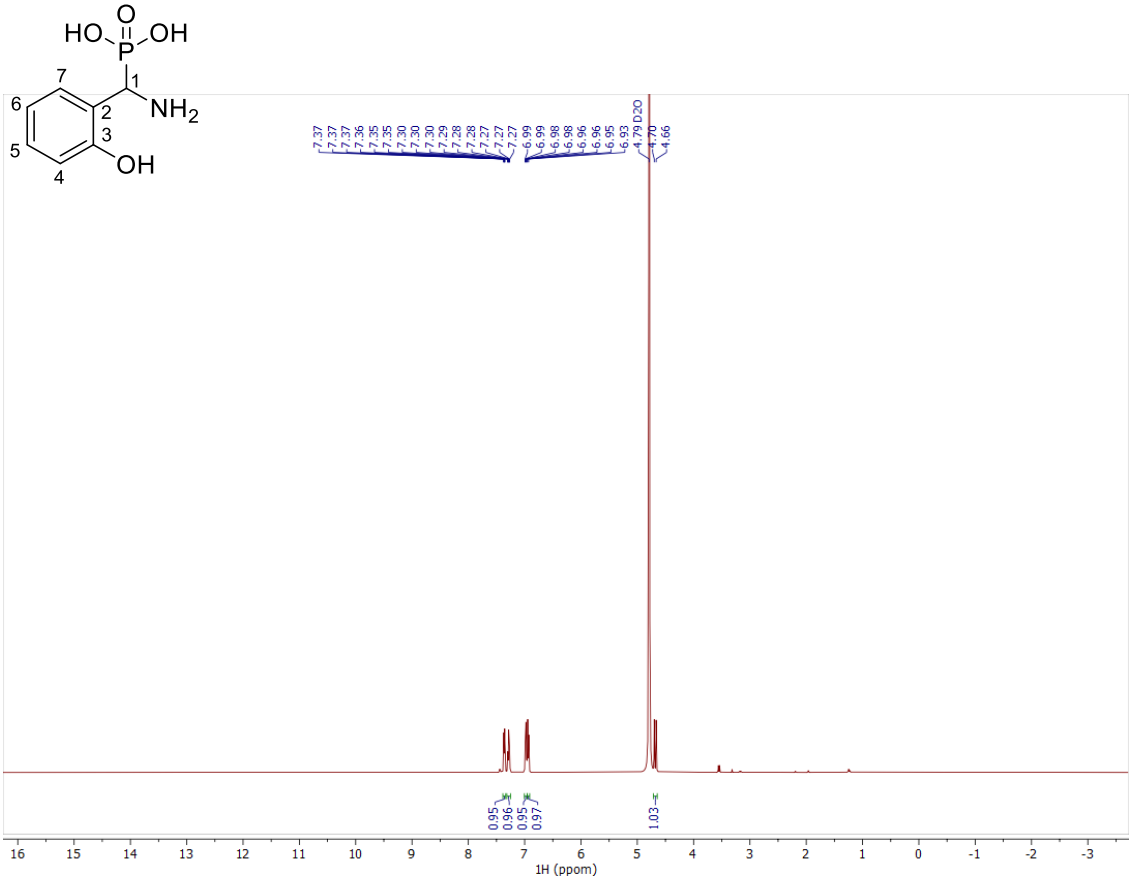

Figure S10. *^{1}H NMR spectrum of **4** (500 MHz, D_2O).*

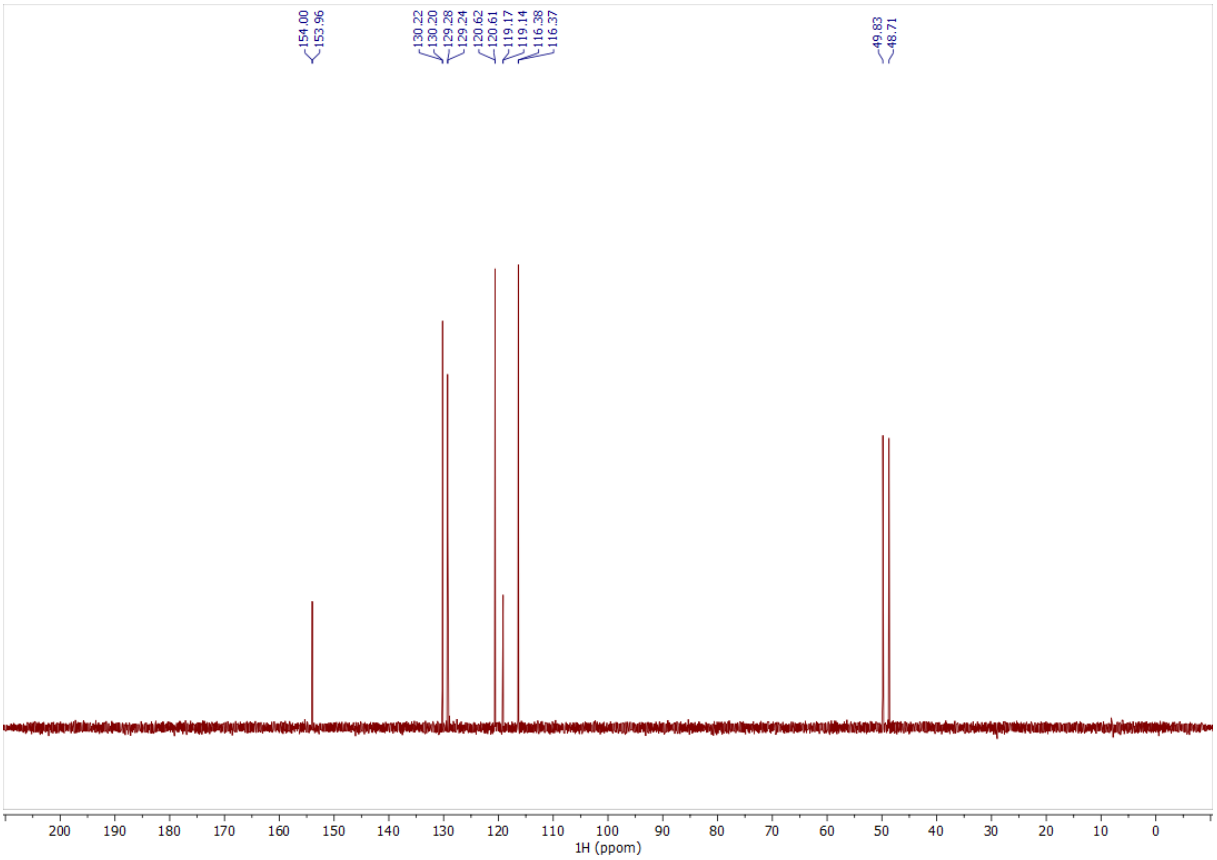

Figure S11. *^{13}C NMR spectrum of **4** (500 MHz, D_2O).*

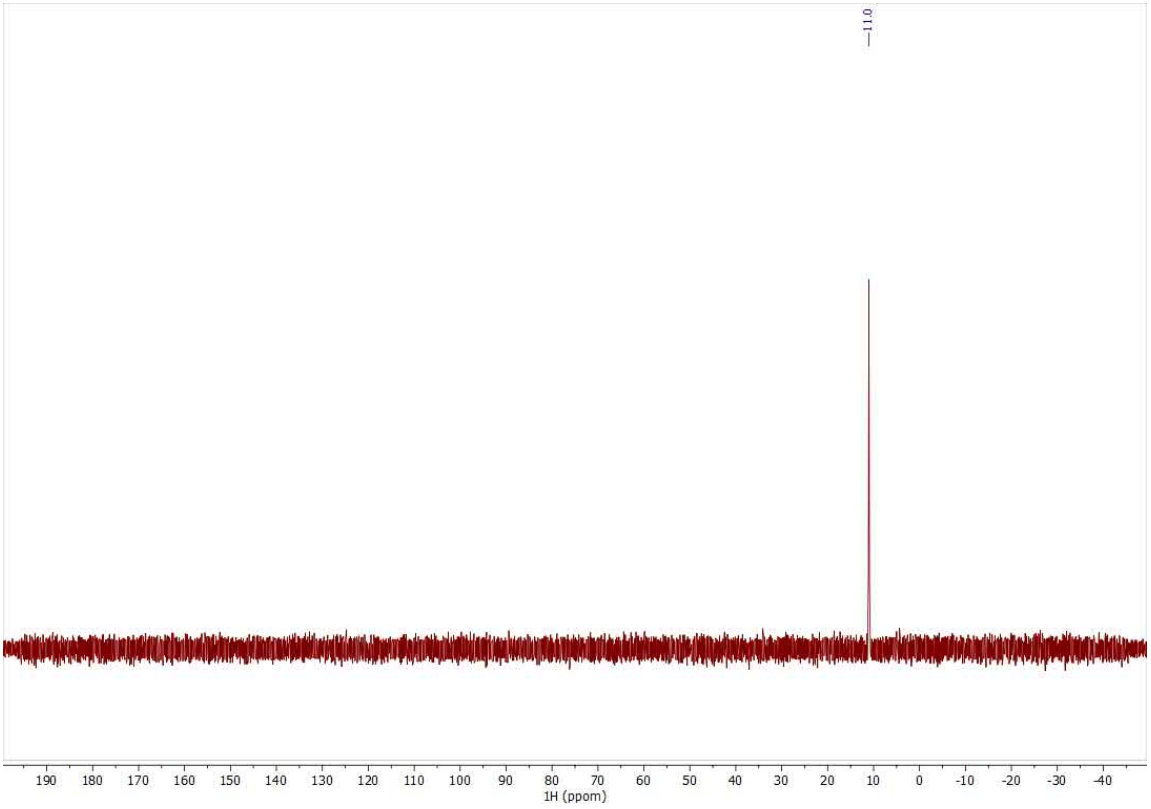

Figure S12. *^{31}P NMR spectrum of **4** (400 MHz, D_2O).*

((Benzylamino)(2-methoxyphenyl)methyl)phosphonic acid (5)

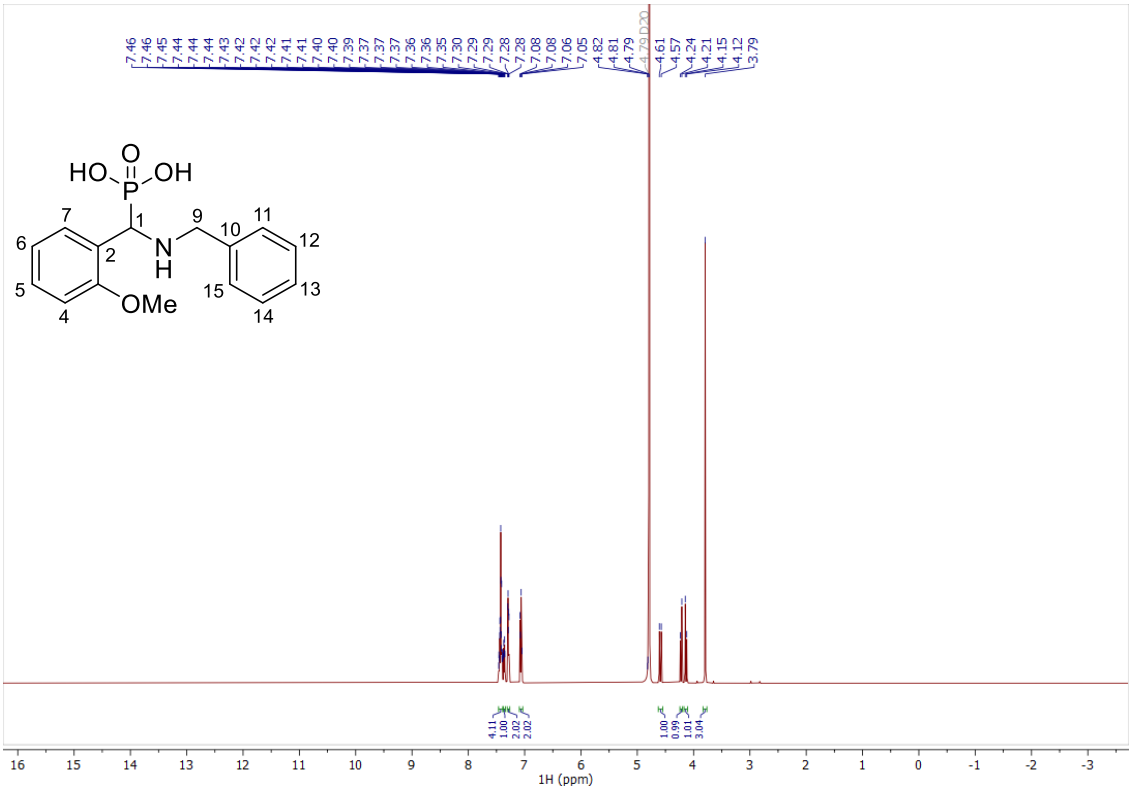

Figure S13. *^{1}H NMR spectrum of **5** (500 MHz, D_2O).*

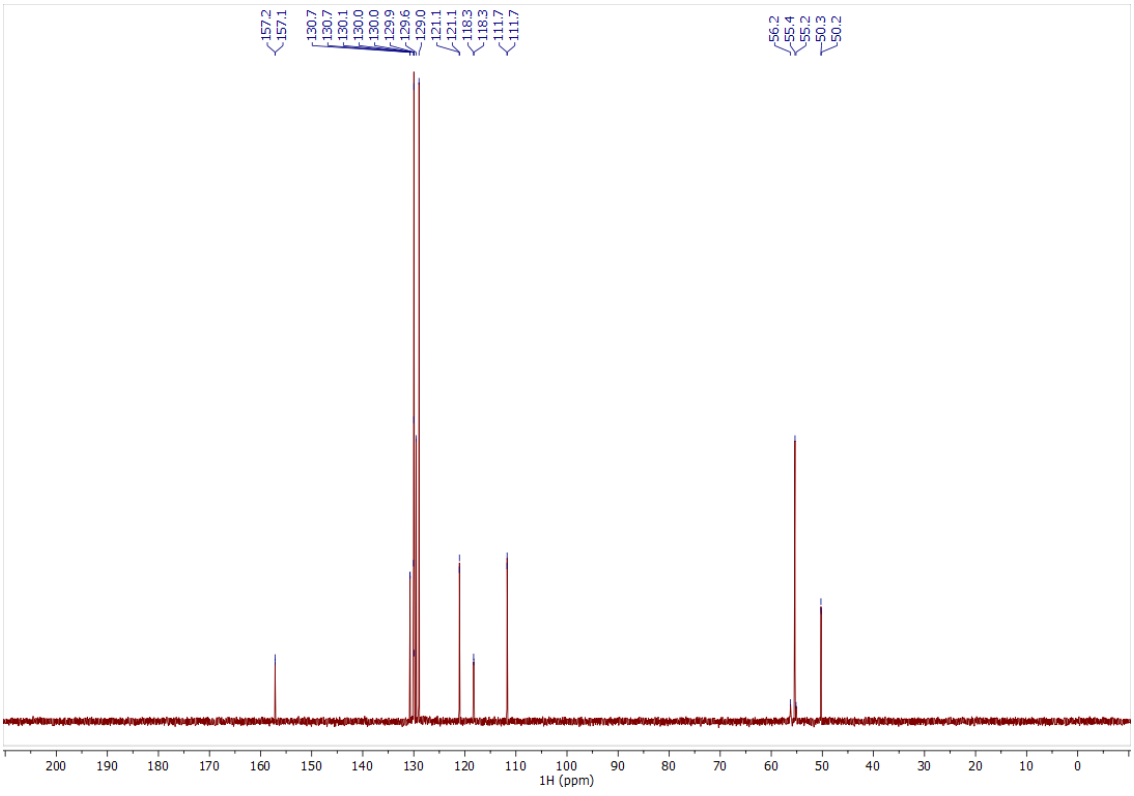

Figure S14. *^{13}C NMR spectrum of **5** (500 MHz, D_2O).*

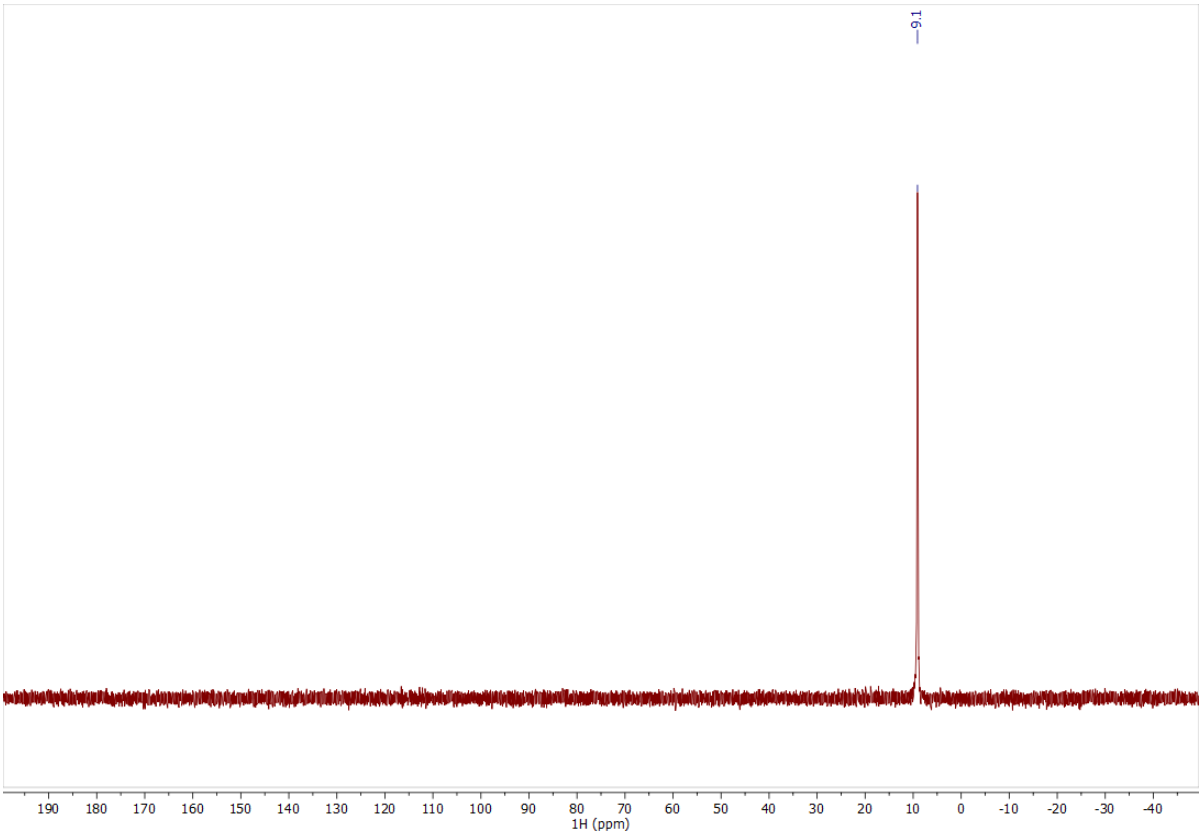

Figure S15. *^{31}P NMR spectrum of **5** (400 MHz, D_2O).*

((Benzylamino)(pyridin-2-yl)methyl)phosphonic acid (6)

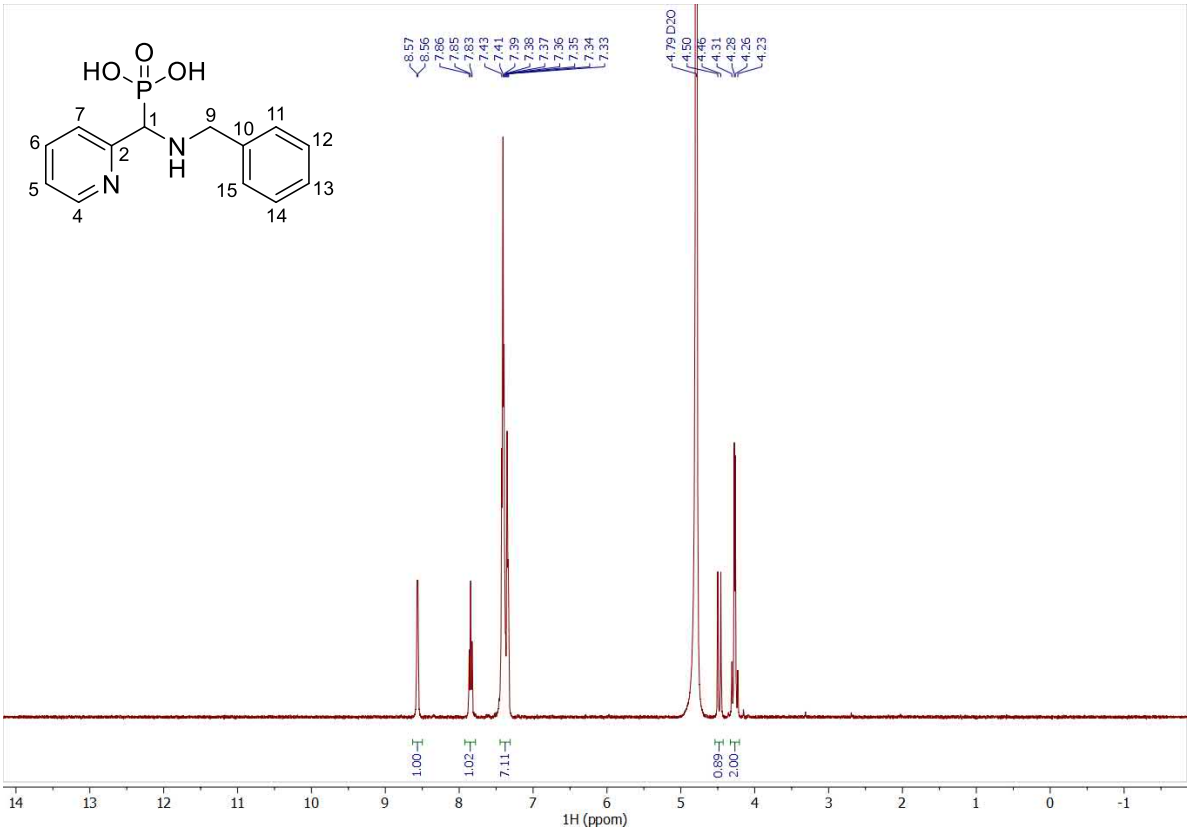

Figure S16. *^{1}H NMR spectrum of **6** (400 MHz, D_2O).*

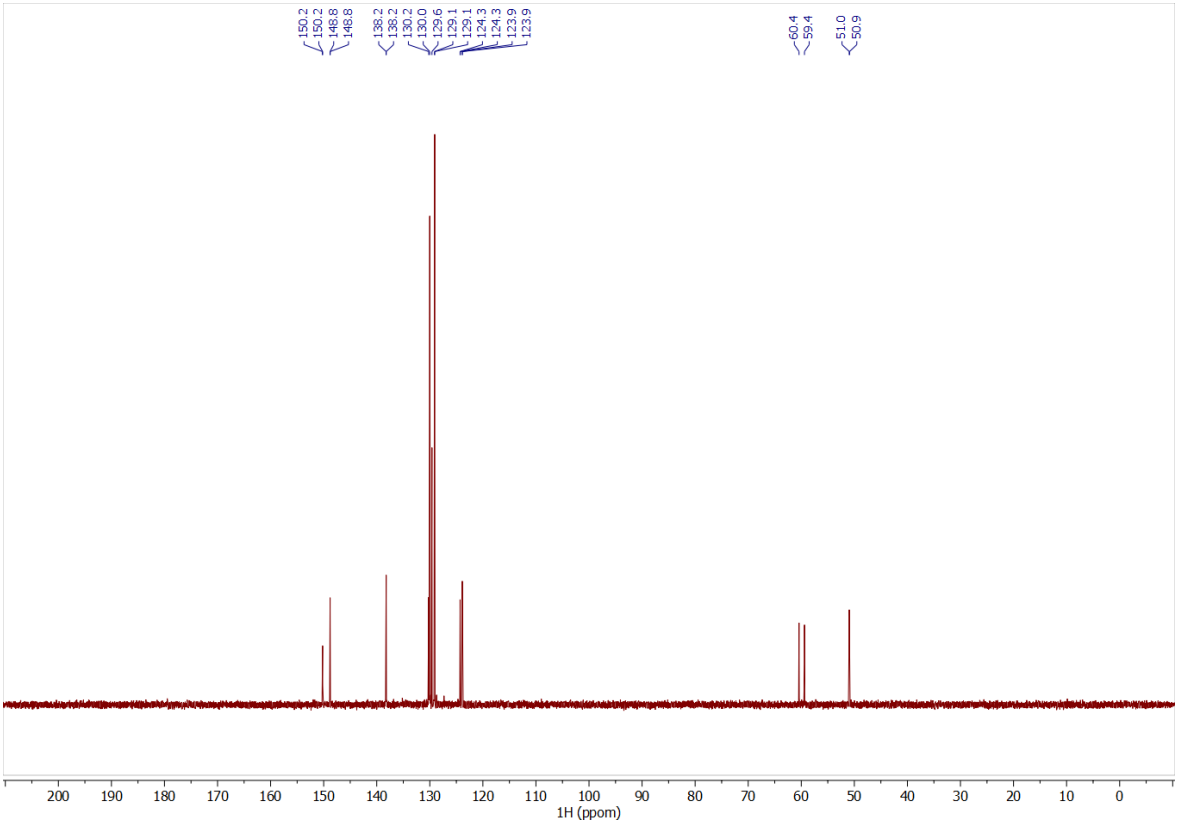

Figure S17. *^{13}C NMR spectrum of **6** (500 MHz, D_2O).*

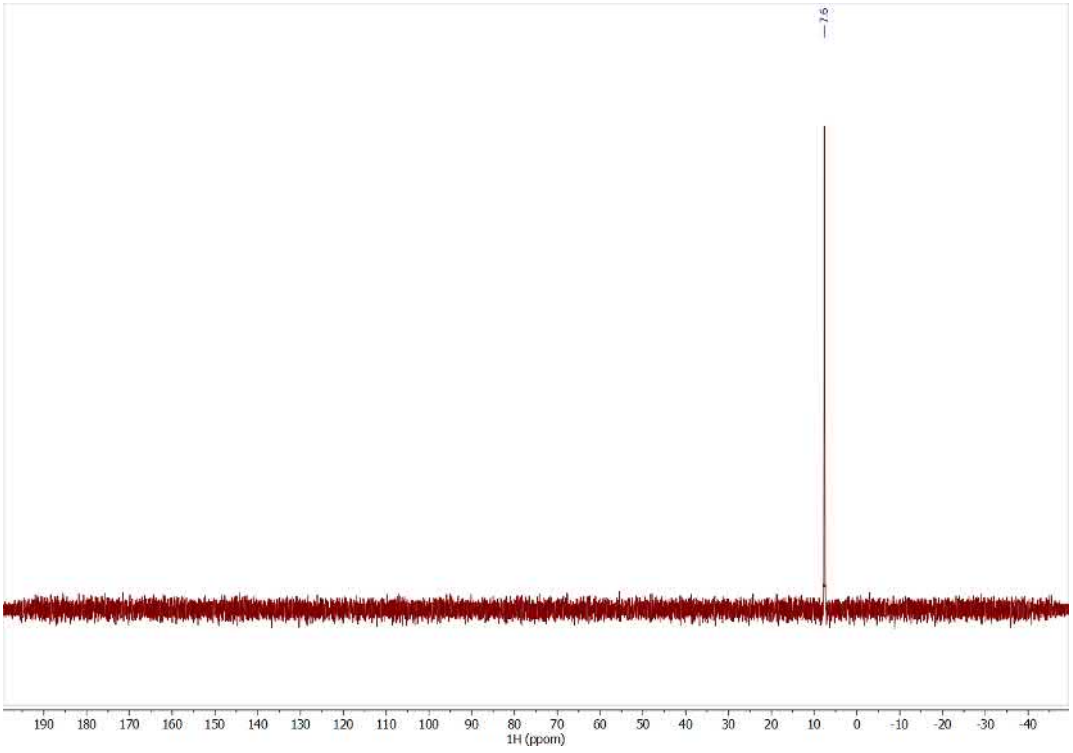

Figure S18. *^{31}P NMR spectrum of **6** (400 MHz, D_2O).*

2. Half-maximal inhibitory concentrations

Table S1. *Measured half-maximal inhibitory concentrations (pIC_{50}) towards VIM-1 (500 pM), VIM-2 (100 pM), NDM-1 (20 pM), IMP-1 (20 pM) and GIM-1 (1.25 nM).*[1]

Inhibitors	***pIC_{50}/IC_{50}* (μM)**				
	VIM-1	**VIM-2**	**NDM-1**	**IMP-1**	**GIM-1**
4	<3/>1000	3.84/144.54	<3/>1000	<3/>1000	<4/>100
5	4.45/35.48	5.07/8.57	<3/>1000	3.27/537.03	<4/>100
6	<3/>1000	3.67/213.80	<3/>1000	3.17/676.08	<4/>100

Table S2. *Dose-response graphs for the enzymatic assay of the inhibitors against VIM-1 (500 pM) and VIM-2 (100 pM).*[1]

Inhibitors	**VIM-1**	**VIM-2**
4	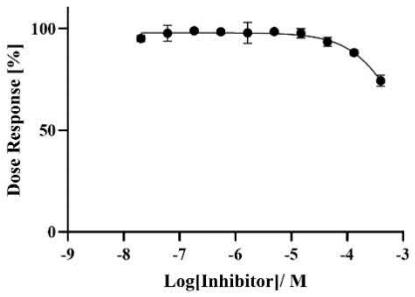	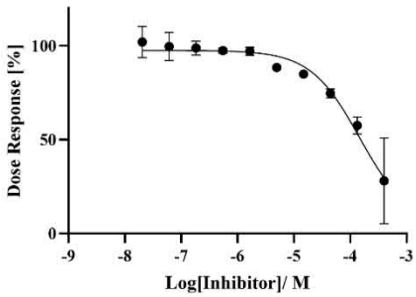
5	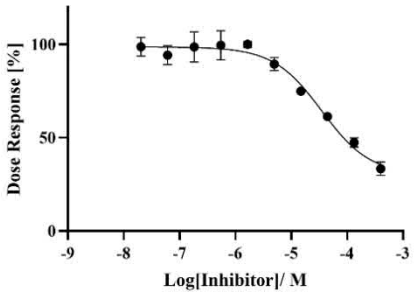	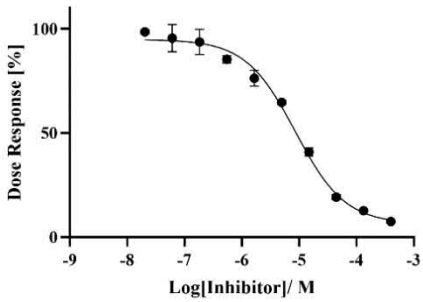
6	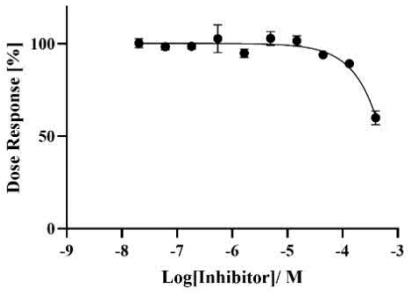	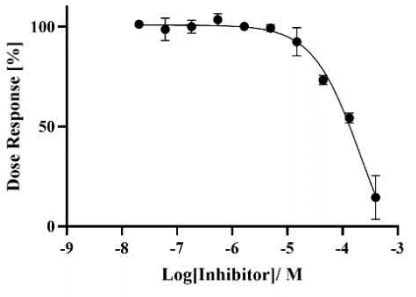

Table S3. *Dose-response graphs from assays of the inhibitors against NDM-1 (50 pM) and IMP-1 (5 pM).* [1]

Inhibitors	NDM-1	IMP-1
4	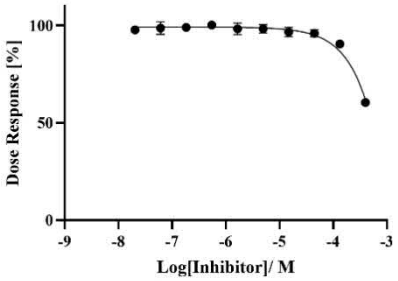	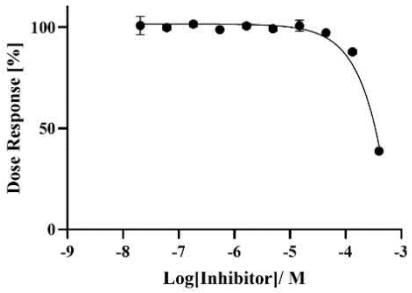
5	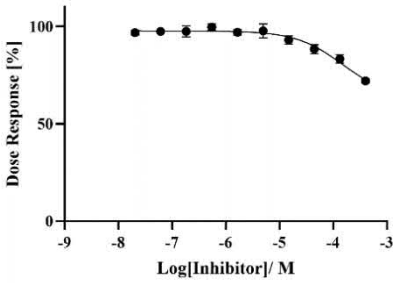	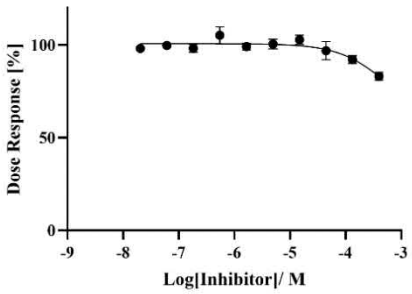
6	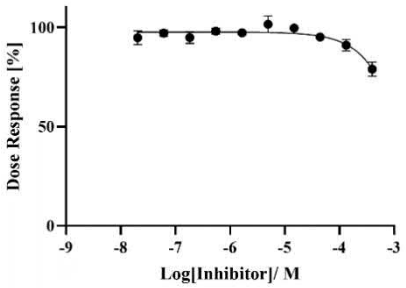	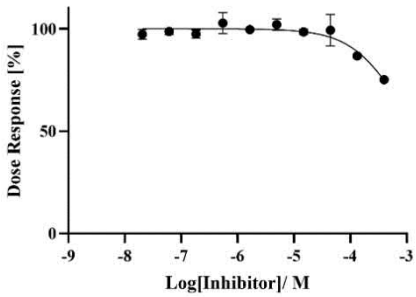

Table S4. *The dose-response graphs from assays of the inhibitors against GIM-1 (1.25 nM).*[1]

Inhibitors	GIM-1
4	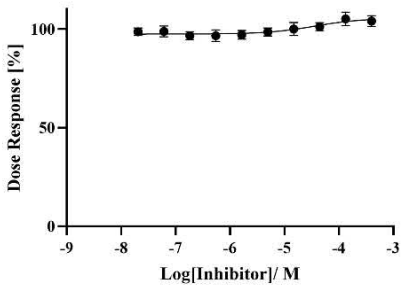
5	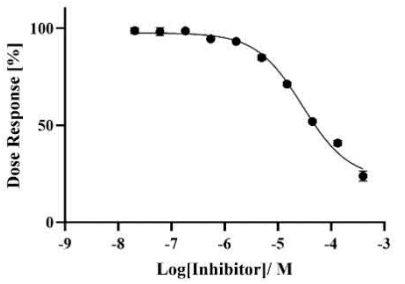
6	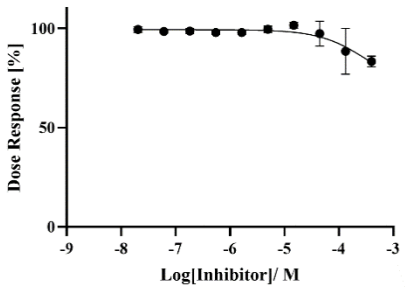

3. Cytotoxicity assays

Table S5. *CC_{50} values and viability curves of metallo-β-lactamase inhibitors were tested using HepG2 cells. CC_{50} values were measured using the MTT assay in a concentration range of 0.0025 mM - 1 mM. Data are shown as % viability values ± SEM (n=4). The calculations were performed using GraphPad Prism software.*

Inhibitors	CC_{50} (mM)	HepG2 viability curves
5	7.5	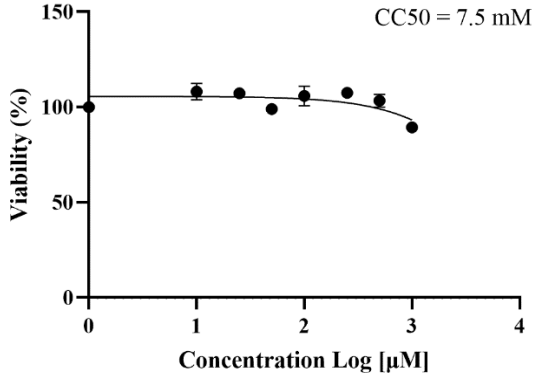
6	3.5	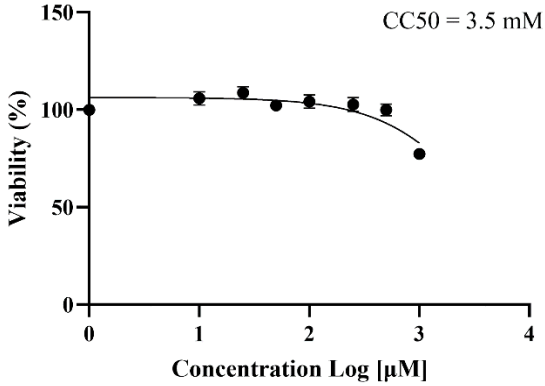

4. NMR titration and chemical shift perturbation

Chemical shift perturbation values were calculated as the weighted average of the chemical shift changes in f1 and f2 dimensions using the following equation[2]:

$$\Delta\delta_{NH} = \sqrt{{\Delta\delta_H}^2 + \left(\frac{\Delta\delta_N}{R_{scale}}\right)^2}\ ;\ R_{scale} = 6.5$$

Table S6. *Chemical shift perturbation for VIM-2 in the presence of compound* ***5****.*

Compound 5	Free VIM-2		VIM-2 in the presence of 10 equiv. of ligand		Difference		CSP
	^{1}H (ppm)	**^{15}N (ppm)**	**^{1}H (ppm)**	**^{15}N (ppm)**	**Δ^{1}H (ppm)**	**Δ ^{15}N (ppm)**	
28D	8.46	123.2	8.46	123.2	0.00	0.0	0.00
29S	8.17	116.1	8.17	116.1	0.00	0.0	0.00
30S	8.43	118.1	8.43	118.1	0.00	0.0	0.00
31G	8.34	110.4	8.34	110.4	0.00	0.0	0.01
32E	8.35	121.0	8.37	121.0	-0.02	0.0	0.02
33Y	8.51	127.6	8.54	127.8	-0.03	-0.2	0.05
35T	7.76	110.7	7.78	110.5	-0.02	0.2	0.04
36V	8.42	116.9					
37S	8.12	111.0	8.13	111.0	-0.01	0.0	0.01
38E	7.62	118.3	7.61	118.2	0.01	0.1	0.02
39I	6.95	119.9	6.88	119.6	0.07	0.4	0.09
43E	7.91	119.1	7.92	119.0	-0.01	0.1	0.02
44V	8.19	115.8	8.17	115.4	0.02	0.5	0.08
45R	8.98	121.9	8.99	121.8	-0.01	0.1	0.02
46L	8.84	119.0					
47Y	9.00	123.5	9.05	124.0	-0.05	-0.5	0.09
48Q	8.63	129.4	8.64	129.4	-0.01	0.0	0.01
49I	8.42	129.7	8.45	129.6	-0.03	0.1	0.03
50A	7.88	119.3	7.91	119.4	-0.03	-0.1	0.03
51D	8.39	119.9	8.40	119.9	-0.01	0.0	0.01
52G	8.14	112.9	8.15	113.0	-0.01	-0.1	0.02
53V	7.21	117.5	7.22	117.5	-0.01	0.0	0.01
54W	9.67	128.5	9.68	128.7	-0.01	-0.2	0.03
55S	9.87	115.4	9.92	115.5	-0.05	-0.1	0.05
56H	7.69	118.6	7.67	118.6	0.02	0.0	0.02
57I	9.04	121.2	9.03	120.9	0.01	0.3	0.04
58A	8.56	128.1	8.58	128.5	-0.02	-0.4	0.06
64G	8.36	104.1	8.40	104.3	-0.04	-0.1	0.05
65A	7.75	124.4	7.75	124.7	0.00	-0.3	0.04
66V	7.85	120.1	7.77	120.2	0.08	-0.1	0.08
67Y	8.86	125.9	8.74	126.0	0.12	-0.2	0.12
69S	9.01	116.0					*
70N	8.49	123.7					*

71G	7.91	106.4					*
72L	8.78	120.5					*
73I	9.48	123.1	9.47	122.8	0.01	0.4	0.05
74V	9.42	126.0	9.43	126.0	-0.01	0.0	0.01
75R	9.26	128.0	9.26	128.0	0.00	0.0	0.00
76D	9.08	129.3	9.08	129.3	0.00	0.0	0.01
77G	8.64	113.3	8.64	113.3	0.00	0.0	0.01
78D	8.86	129.6	8.86	129.5	0.00	0.1	0.01
79E	7.61	116.8	7.61	116.8	0.00	0.0	0.00
80L	8.69	116.5	8.69	116.5	0.00	0.0	0.00
81L	8.84	123.4	8.83	123.3	0.01	0.0	0.01
82L	8.83	128.4	8.84	128.3	-0.01	0.2	0.03
83I	9.57	126.7	9.57	126.6	0.00	0.1	0.02
84D	8.99	118.8	9.03	118.9	-0.04	0.0	0.04
85T	6.70	104.1	6.54	103.7	0.16	0.4	0.17
97A	7.48	122.0	7.42	121.9	0.06	0.0	0.06
98E	8.40	122.1	8.41	121.8	-0.01	0.3	0.04
99I	8.50	119.7	8.54	119.8	-0.04	-0.1	0.04
100E	7.64	122.6	7.63	122.6	0.01	0.0	0.01
101K	7.43	116.1	7.41	116.1	0.02	0.0	0.02
102Q	8.34	113.3	8.37	113.4	-0.03	-0.1	0.04
103I	8.04	117.3	7.97	117.2	0.07	0.1	0.07
104G	8.20	104.8	8.23	104.9	-0.03	0.0	0.03
105L	6.11	117.0	6.11	117.1	0.00	0.0	0.01
107V	8.74	122.3	8.74	122.3	0.00	0.0	0.01
108T	8.33	114.2	8.34	114.1	-0.01	0.0	0.01
109R	7.54	121.4	7.53	121.3	0.01	0.1	0.02
110A	8.93	121.8	8.93	121.8	0.00	0.0	0.00
111V	8.72	120.9	8.70	120.9	0.02	0.0	0.02
112S	7.65	122.0	7.69	122.1	-0.04	-0.1	0.04
124D	7.68	117.5	7.66	117.4	0.02	0.1	0.03
125V	7.66	123.6	7.67	123.7	-0.01	0.0	0.01
126L	7.62	118.5					
127R	8.77	121.4	8.78	120.8	-0.01	0.7	0.10
128A	7.98	122.9	7.99	122.9	-0.01	0.0	0.01
129A	7.39	119.6	7.40	119.6	-0.01	0.0	0.01
130G	7.82	106.5	7.81	106.5	0.01	0.0	0.01
131V	7.91	121.9	7.95	122.0	-0.04	-0.2	0.05
132A	7.85	131.8	7.86	131.8	-0.01	0.0	0.01
133T	8.24	116.1	8.25	116.2	-0.01	-0.1	0.02
134Y	9.10	120.1	9.12	120.2	-0.02	-0.1	0.02
135A	8.64	118.4	8.66	118.4	-0.02	-0.1	0.02
136S	10.24	119.3	10.25	119.3	-0.01	0.0	0.01
138S	7.56	112.9	7.60	113.0	-0.04	-0.1	0.04
139T	8.16	121.0	8.16	121.0	0.00	0.0	0.00
140R	8.23	117.7	8.20	117.7	0.03	0.0	0.03
141R	7.69	119.3	7.68	119.3	0.01	0.0	0.01
142L	8.01	119.9	8.02	119.9	-0.01	0.0	0.01
143A	8.54	120.7	8.54	120.7	0.00	0.0	0.01
144E	7.55	118.1	7.51	118.1	0.04	0.0	0.04

145V	7.98	120.2	7.97	120.2	0.01	0.0	0.01
146E	7.67	117.6	7.70	117.7	-0.03	0.0	0.03
147G	7.71	106.1	7.71	106.1	0.00	0.0	0.01
148N	8.15	119.8	8.17	119.8	-0.02	0.0	0.02
149E	8.09	119.7					
150I	8.06	115.6	8.10	115.5	-0.04	0.0	0.04
152T	8.46	122.7	8.47	122.7	-0.01	0.0	0.01
153H	8.76	118.4	8.76	118.3	0.00	0.0	0.01
154S	8.63	116.6	8.64	116.8	-0.01	-0.1	0.02
155L	7.90	125.9	7.92	125.9	-0.02	0.0	0.02
156E	8.33	122.6	8.35	122.7	-0.02	-0.1	0.02
157G	8.21	106.5	8.22	106.5	-0.01	0.0	0.01
158L	8.11	119.5	8.11	119.5	0.00	0.0	0.00
159S	8.42	114.7	8.41	114.6	0.01	0.1	0.02
160S	8.93	119.2	8.93	119.3	0.00	0.0	0.01
161S	8.68	120.4	8.68	120.4	0.00	0.0	0.00
162G	8.86	112.9	8.85	112.9	0.01	0.0	0.01
163D	8.01	123.7	8.01	123.7	0.00	0.0	0.00
164A	7.93	120.6	7.93	120.6	0.00	0.0	0.00
165V	9.00	116.7	9.00	116.8	0.00	-0.1	0.01
166R	8.77	125.0	8.78	125.0	-0.01	0.0	0.01
167F	8.92	130.1	8.92	130.3	0.00	-0.2	0.03
168G	8.42	115.0					
170V	7.52	110.6	7.52	110.6	0.00	0.0	0.00
171E	9.53	121.8	9.54	121.8	-0.01	0.0	0.01
172L	9.25	124.8	9.25	124.8	0.00	0.0	0.01
173F	8.93	122.7	8.92	122.7	0.01	0.0	0.01
174Y	8.45	127.7	8.47	127.8	-0.02	0.0	0.02
177A	7.95	117.5	7.97	117.7	-0.02	-0.2	0.04
178A	7.36	123.3	7.29	123.1	0.07	0.1	0.07
179H	6.18	124.4	6.23	124.3	-0.05	0.0	0.05
180S	7.66	107.4	7.68	107.4	-0.02	0.0	0.02
181T	9.67	115.0	9.72	115.1	-0.05	-0.1	0.05
182D	10.11	117.4	10.08	117.5	0.03	-0.1	0.03
183N	6.45	116.2	6.46	116.2	-0.01	0.0	0.01
184L	8.87	119.7	8.84	119.7	0.03	0.0	0.03
185V	9.10	113.3	9.09	113.3	0.01	0.0	0.01
186V	8.50	119.4	8.48	119.3	0.02	0.1	0.03
187Y	9.59	128.6	9.58	128.6	0.01	0.0	0.01
188V	8.62	126.8	8.65	126.9	-0.03	0.0	0.03
190S	7.68	113.1	7.67	112.9	0.01	0.2	0.03
191A	6.53	120.7	6.53	120.7	0.00	0.0	0.00
192S	7.55	112.0	7.55	112.1	0.00	-0.1	0.01
193V	6.57	116.9	6.57	116.9	0.00	0.0	0.01
194L	9.36	129.1	9.33	129.0	0.03	0.0	0.03
195Y	10.02	128.7	10.04	128.4	-0.02	0.3	0.04
196G	8.62	112.0	8.57	111.5	0.05	0.5	0.09
199A	6.52	115.6	6.49	115.3	0.03	0.3	0.05
200I	7.06	113.4	6.98	113.3	0.08	0.1	0.08
201Y	8.99	129.0					*

202E	8.52	116.4					*
203L	8.32	121.3	8.48	122.0	-0.16	-0.7	0.19
204S	8.51	108.7	8.39	108.7	0.12	0.0	0.12
205R	7.61	124.7	7.69	124.7	-0.08	0.0	0.08
206T	8.29	114.7					*
207S	7.46	115.9					*
208A	8.63	124.5	8.28	125.7	0.35	-1.2	0.39
209G	7.50	105.9	7.19	105.9	0.31	0.0	0.31
211V	8.47	119.4	8.47	120.0	0.00	-0.5	0.08
212A	8.16	127.0					*
213D	7.91	114.3	8.21	112.9	-0.30	1.4	0.37
214A	7.15	122.2	6.92	122.2	0.23	-0.1	0.23
215D	7.87	118.9	7.85	119.0	0.02	-0.2	0.03
216L	8.63	122.5	8.48	122.0	0.15	0.4	0.16
217A	7.85	118.8	7.83	118.7	0.02	0.0	0.02
218E	7.60	117.9	7.60	117.9	0.00	-0.1	0.01
221T	7.41	117.9	7.39	117.9	0.02	0.0	0.02
222S	8.86	122.5	8.87	122.4	-0.01	0.1	0.02
223I	8.26	120.7	8.24	120.6	0.02	0.0	0.02
224E	7.86	122.0	7.86	122.1	0.00	0.0	0.01
225R	8.11	117.9	8.10	117.9	0.01	0.0	0.01
226I	7.78	119.1	7.77	119.1	0.01	0.0	0.01
227Q	8.32	119.2	8.30	119.2	0.02	0.0	0.02
228Q	8.05	113.7	8.05	113.7	0.00	0.0	0.01
229H	7.50	117.0	7.50	116.9	0.00	0.1	0.01
230Y	7.46	115.2	7.45	115.1	0.01	0.1	0.01
232E	8.37	117.2	8.37	117.2	0.00	0.0	0.00
233A	7.05	122.1	7.05	122.1	0.00	0.0	0.00
234Q	8.67	120.8	8.66	120.7	0.01	0.0	0.01
235F	7.55	117.6	7.56	117.8	-0.01	-0.2	0.03
236V	9.10	125.1	9.09	125.1	0.01	-0.1	0.02
237I	9.12	126.8	9.23	126.8	-0.11	0.0	0.11
239G	7.35	108.4	7.45	108.2	-0.10	0.2	0.10
240H	7.45	114.6					*
241G	9.27	112.2					*
242L	7.66	119.0					*
244G	8.46	109.4	8.47	109.3	-0.01	0.1	0.02
245G	8.38	115.1	8.39	115.1	-0.01	0.0	0.01
246L	8.79	120.9	8.78	121.0	0.01	0.0	0.01
247D	9.47	120.5	9.46	120.5	0.01	0.0	0.01
248L	8.26	120.7	8.24	120.6	0.02	0.0	0.02
249L	8.08	122.8	8.06	122.9	0.02	-0.1	0.02
250K	6.83	119.9	6.72	120.0	0.11	-0.1	0.11
251H	8.09	117.5	8.09	117.6	0.00	0.0	0.01
252T	7.82	114.2	7.76	114.0	0.06	0.2	0.07
253T	7.61	116.8	7.61	116.8	0.00	0.0	0.00
254N	7.74	119.4	7.71	119.3	0.03	0.1	0.04
255V	7.93	121.3	7.88	120.8	0.05	0.5	0.09
256V	8.02	119.1	7.92	119.0	0.10	0.1	0.10
257K	8.35	119.6	8.30	119.5	0.05	0.1	0.05

258A	7.59	120.5	7.55	120.6	0.04	-0.1	0.04
259H	7.69	118.6	7.67	118.6	0.02	0.0	0.02
260T	7.68	112.6	7.67	112.4	0.01	0.2	0.03
261N	8.04	120.4	8.08	120.5	-0.04	-0.1	0.04
262R	7.92	120.9	8.00	120.8	-0.08	0.0	0.08
263S	8.23	116.9	8.22	116.9	0.01	0.0	0.01
264V	8.02	121.8	8.01	121.7	0.01	0.1	0.02
265V	8.14	124.3	8.12	124.3	0.02	0.0	0.02
266E	7.94	130.2	7.93	130.2	0.01	0.0	0.01

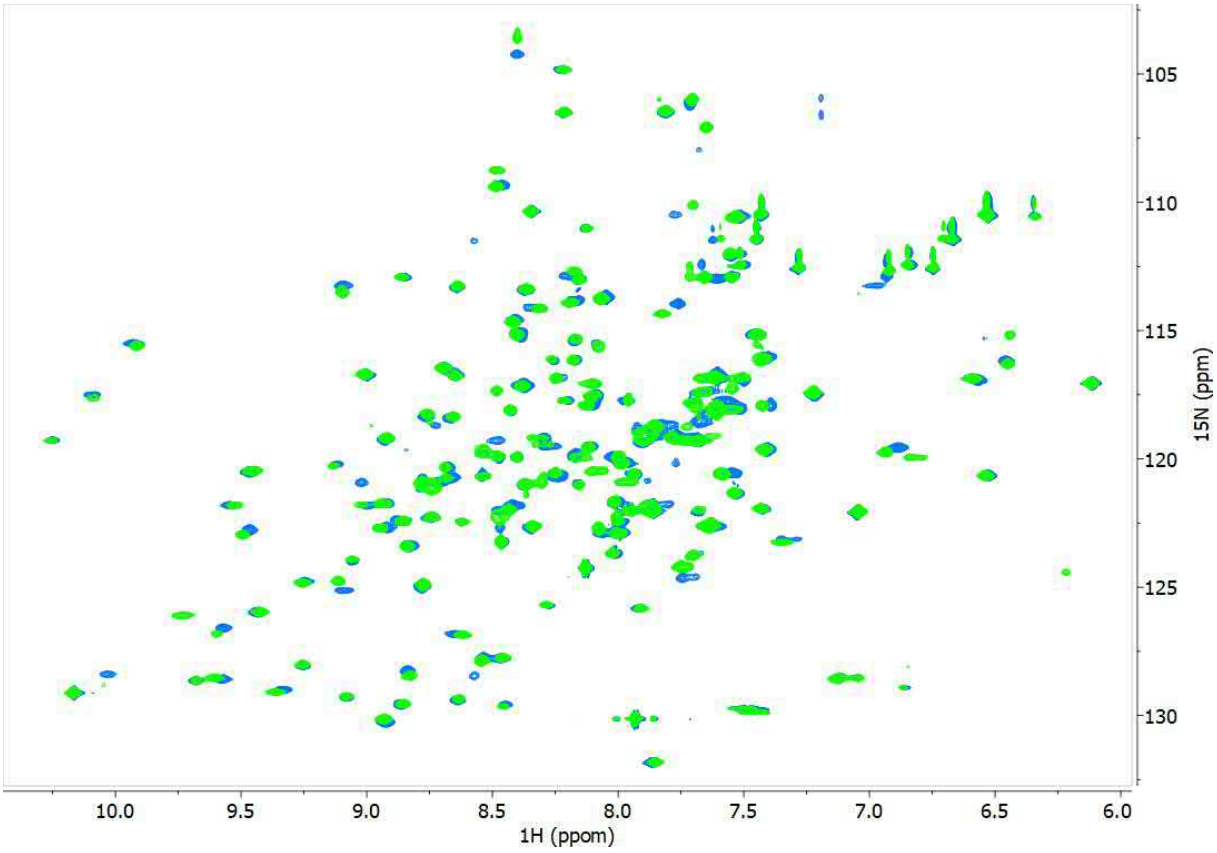

Figure S16. *Superimposition of the $^{1}H,^{15}N$-HSQC spectra (600 MHz, pH 7.0, 25 °C) of VIM-2 in the presence of 10 molar equivalents of compound* ***5*** *(blue) and in the presence of 10 molar equivalents of compound* ***5j***[3] *(green). The data suggests that the two compounds bind in the same pocket close to the zinc ions, but that the binding of compound* ***5*** *is relatibvely shifted towards the Zn2 site while the CSPs of residues both around the Zn1 and Zn2 site in the case of compound* ***5j*** *indicate its location between the two zinc ions.*

5. X-ray diffraction

Table S7. *Data-collection and refinement statistics. Values for highest resolution shell are in brackets.*

Ligand	**5**
PDB ID	**29GW**
Data collection	
Beam size (FWHM µm)	50x50
Flux (ph/s)	5.288 E+11
Energy (keV)	12.7
Exposure time per frame (ms)	10
Diffraction weighted dose (MGy)	0.787099
Number of images	2000
SpaceGroup	C2
Unit cell constants	101.422, 79.295, 67.631
Unit cell angles	90.0, 130.325, 90.0
Resolution	39.65 - 1.4 (1.43 – 1.4)
R_{merge}	0.047 (0.307)
R_{meas}	0.055 (0.356)
R_{pim}	0.027 (0.176)
Total number of observations	301567 (14915)
Unique number of observations	77552 (878)
Mean I/sd(I)	14.5 (3.1)
Completeness (ellipsoidal)	97.7 (87.2)
Multiplicity	3.9 (3.8)
$CC_{1/2}$	0.998 (0.919)
Refinement	
Resolution range	33.80 - 1.40
Number of reflections	77547
R_{work}	0.1643
R_{free}	0.1829
Test set size (%)	5.03
Wilson B ($Å^2$)	10.93

Deviations from ideal values	
Bonds	0.010
Angles	1.038
Ramachandran Plot	
Outliers (%)	0.44
Allowed (%)	1.31
Favoured (%)	98.26
mean B-factors	
Overall	16.08
Protein	14.55
Water	27.30
Other	22.82

Table S8. *Comparison of VIM-2: inhibitor complexes with* ***5*** *and* ***5j*** *with the structure of apo VIM-2.*

PBD-ID	**ligand**	**Space group**	**Orientation molecules in ASU**	**r.m.s.d. (Å)**				
				Intramolecular	**Apo (5YD7)**		**Inhibitor 5**	
					Chain A	**Chain B**	**Chain A**	**Chain B**
29GW	5	C2	Face-to-back	0.18	0.12	0.14	n.a.	n.a.
9F0S	5j	C2	Face-to-back	0.16	0.11	0.12	0.07	0.09

Table S9. *Nature of inhibitor* ***5*** *binding to VIM-2 (PDB 29GW).*

	VIM-2 inhibitor 5 complex	
	Chain A	**Chain B**
Enantiomer	R	S/R
Occupancy	0.85	0.31/0.33
RSCC	0.94	0.80/0.80

Table S10. *Comparison of selected Cα positions between the inhibitor* ***5****: VIM-2 complex and apo VIM-2 PDB 29GW and 5YD7).*

	Inhibitor 5 induced Cα shift compared to apo VIM-2 (Å)				
	Phe62	**Asp63**	**Gly209**	**Asn210**	**Ala212**
Chain A	1.0	0.8	0.5	0.5	0.6
Chain B	0.5	0.9	0.2	0.2	0.2

6. ADME predictions

Table S11. *Physicochemical properties of compounds* ***4-6****.*

Compound	**4**	**5**	**6**
Formula	$C_7H_{10}NO_4P$	$C_{15}H_{18}NO_4P$	$C_{13}H_{15}N_2O_3P$
MW [g/mol]	203.13	307.28	278.24
Nr. of heavy atoms	13	21	19
Nr. of aromatic heavy atoms	6	12	12
Nr. of H-bond acceptors	5	5	5
Nr. of H-bond donors	4	3	3
Molar Refractivity	47.13	80.98	72.29
Nr. of rotatable bonds	2	6	5
TPSA [Å^2][4]	113.59	88.60	92.26

Table S12. *SwissADME predictions of compounds* ***4-6****.*

Compound	**4**	**5**	**6**
Consensus Log $P_{o/w}$[a]	-0.93	0.94	0.24
Water Solubility[b]	Highly soluble/ Soluble	Very soluble/ Moderately soluble	Highly soluble/ Soluble
BBB permeant	No	No	No
Pgp substrate	No	No	No
CYP3A4 inhibitor	No	No	No
CYP2D6 inhibitor	No	No	No
CYP2C19 inhibitor	No	No	No
CYP2C9 inhibitor	No	No	No
CYP1A2 inhibitor	No	No	No
GI absorption	High	High	High

a, Average of the 5 predicted Log $P_{o/w}$ values predicted by the SwissADME webserver (iLogP[5], XlogP3 [XLOGP program, version 3.2.2], WlogP[6], MlogP[7-9], SILICOS-IT [FILTER-IT program, version 1.0.2]). ***b,*** According to the three Log*S* values predicted by the SwissADME webserver (ESOL[10], Ali[11], SILICOS-IT [FILTER-IT program, version 1.0.2]).

Table S13. *PreADME predictions for compounds* ***4-6****.*

Compound	**4**	**5**	**6**
Water solubility [mg/L]	244964	8888	86610
logP	0.25	2.17	1.31
BBB penetration	0.121	0.511	0.325
HIA [%][12]	43.3	91.9	87.3
Pgp inhibition	Non	Non	Non
CYP3A4 inhibition	Non	Non	Non
CYP2D6 inhibition	Inhibitor	Inhibitor	Inhibitor
CYP2C19 inhibition	Non	Non	Non
CYP2C9 inhibition	Inhibitor	Inhibitor	Inhibitor
Caco-2 permeability	0.885	0.826	0.718
MDCK permeability	2.3	232.9	188.2
PPB [%]	12.9	82.7	70.1

7. Recombinant protein production and purification

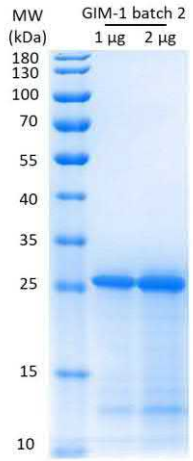

Figure S17*. SDS-PAGE gel analysis of 1 and 2 µg of GIM-1 batch 2*. PageRuler Prestained Protein Ladder (Thermo Scientific, product # 26616).

8. Additional figures

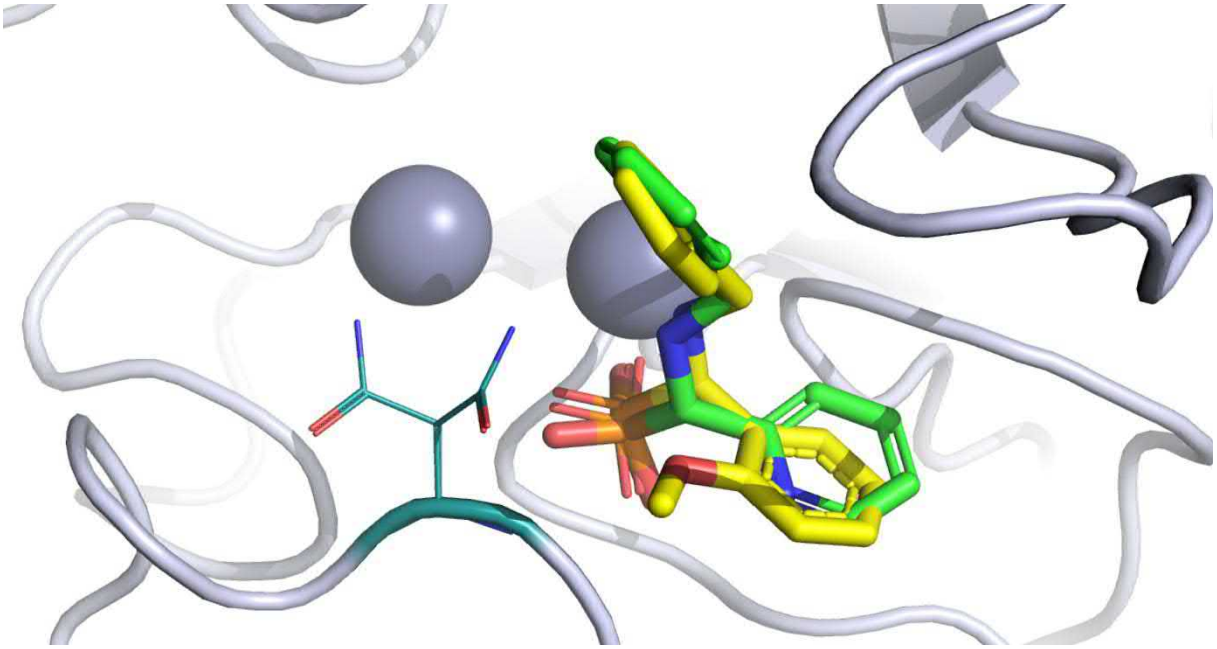

Figure S18*. View from the overlaid structure of* ***5*** *(X-ray, PDB 29GW) and* ***6*** *(molecular docking) in the binding site of VIM-2. The low inhibitory potency of* ***6*** *against VIM-1 and VIM-2 may be rationalized by loss of hydrogen bonding to Asn210 compared to analogue* ***5****.*

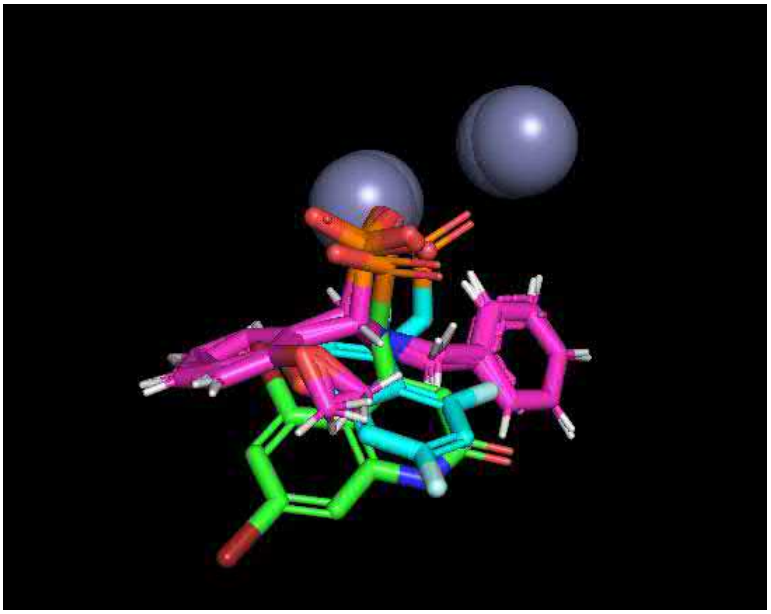

***Figure S19**. View from the superimposed crystal structures of **5** (magenta, PDB 29GW) and heteroaryl phosphonates and hetteroaryl phosphonnates (PDB ID 6NY7, green; PDB ID 6DD0, cyan)[12] in the VIM-2 binding site. Similar to **5**, heteroaryl phosphonnates also bind Zn2 of the active site.*

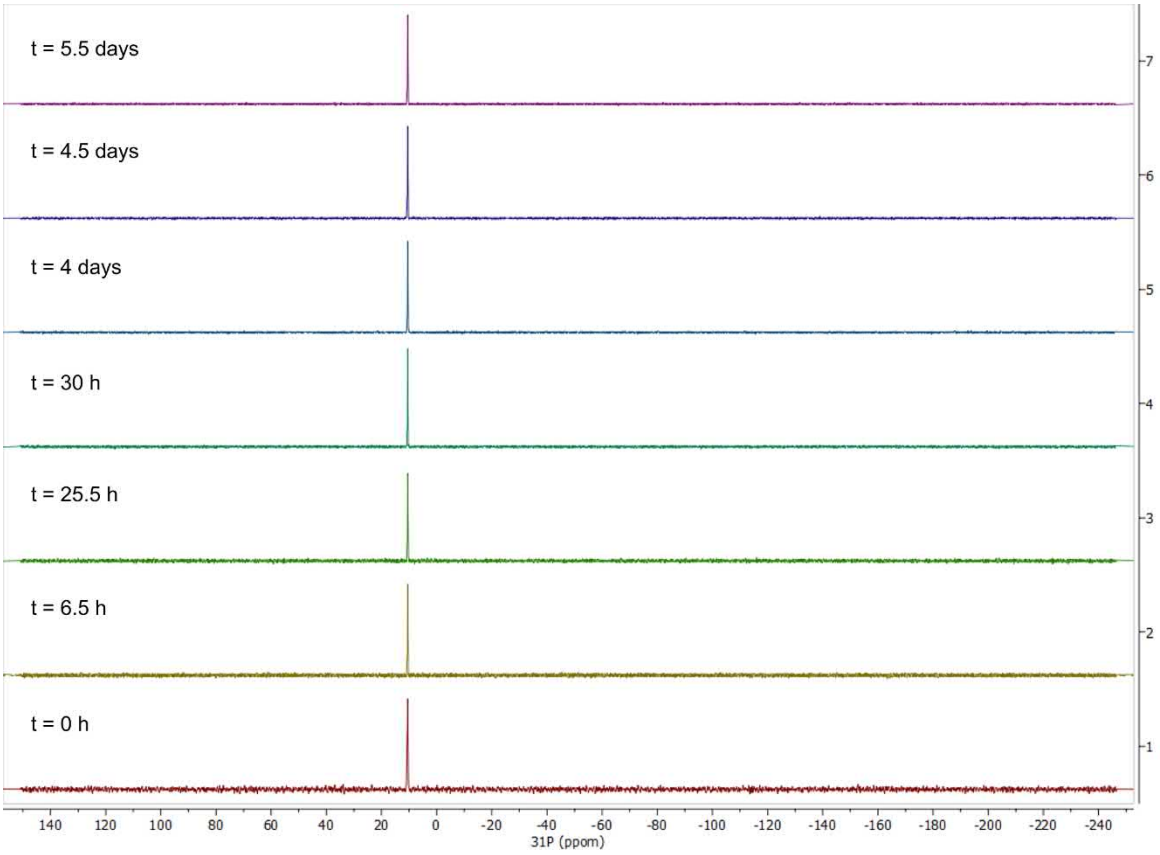

***Figure S20**. ^{31}P NMR spectra acquired for **5** under the conditions comparable to that used for their co-crystallization with VIM-2 (0.2 M MgCl2, 50 mM HEPES, 15 % (v/v) ethylene glycol, 25 % (w/v) PEG2000 in D_2O, pH 7.2).*

9. References

1. van Berkel, S.S. et al. Assay platform for clinically relevant metallo-beta-lactamases. *J Med Chem* **56**, 6945-53 (2013).
2. Mulder, F.A.A., Schipper, D., Bott, R. & Boelens, R. Altered flexibility in the substrate-binding site of related native and engineered high-alkaline Bacillus subtilisins. *J. Mol. Biol.* **292**, 111-123 (1999).
3. Gulyás, K.V. et al. Dynamically chiral phosphonic acid-type metallo-β-lactamase inhibitors. *Commun. Chem.* **8**, 119 (2025).
4. Ertl, P., Rohde, B. & Selzer, P. Fast Calculation of Molecular Polar Surface Area as a Sum of Fragment-Based Contributions and Its Application to the Prediction of Drug Transport Properties. *J. Med. Chem.* **43**, 3714–3717 (2000).
5. Daina, A., Michielin, O. & Zoete, V. iLOGP: A Simple, Robust, and Efficient Description of n-Octanol/Water Partition Coefficient for Drug Design Using the GB/SA Approach. *J. Chem. Inf. Model.* **54**, 3284–3301 (2014).
6. Wildman, S.A. & M., C.G. Prediction of Physicochemical Parameters by Atomic Contributions. *J. Chem. Inf. Comput. Sci.* **39**, 868–873 (1999).
7. Moriguchi, I., Hirono, S., Nakagome, I. & Hirano, H. Comparison of Reliability of Log P Values for Drugs Calculated by Several Methods. *Chem. Pharm. Bull.* **42**, 976-978 (1994).
8. Lipinski, C.A., Lombardo, F., Dominy, B.W. & Feeney, P.J. Experimental and computational approaches to estimate solubility and permeability in drug discovery and development settings. *Adv. Drug. Deliv. Rev.* **23**, 3-25 (1997).
9. Moriguchi, I., Hirono, S., Liu, Q., Nakagome, I. & Matsushita, Y. Simple method of calculating octanol/water partition coefficient. *Chem. Pharm. Bull.* **40**, 127–130 (1992).
10. Delaney, J.S. ESOL: Estimating Aqueous Solubility Directly from Molecular Structure. *J. Chem. Inf. Comput. Sci.* **44**, 1000–1005 (2004).
11. Ali, J., Camilleri, P., Brown, M.B., Hutt, A.J. & Kirton, S.B. In Silico Prediction of Aqueous Solubility Using Simple QSPR Models: The Importance of Phenol and Phenol-like Moieties. *J. Chem. Inf. Model.* **52**, 2950–2957 (2012).
12. Zhao, Y.H. et al. Evaluation of human intestinal absorption data and subsequent derivation of a quantitative structure-activity relationship (QSAR) with the Abraham descriptors. *J. Pharm. Sci.* **90**, 749-784 (2001).